Microbiology (2016), **162**, 2005–2016 DOI 10.1099/mic.0.000369

Loop structures in the 5′ untranslated region and antisense RNA mediate *pilE* gene expression in *Neisseria gonorrhoeae*

Thao L. Masters, Jenny Wachter and Stuart A. Hill

Department of Biological Sciences, Northern Illinois University, DeKalb, IL 60115, USA

Correspondence
Stuart A. Hill
sahill@niu.edu

Received 18 May 2016
Accepted 31 August 2016

Regulation of the *Neisseria gonorrhoeae pilE* gene is ill-defined. In this study, post-transcriptional effects on expression were assessed. *In silico* analysis predicts the formation of three putative stable stem–loop structures with favourable free energies within the 5′ untranslated region of the *pilE* message. Using quantitative reverse transcriptase PCR analyses, we show that each loop structure forms, with introduced destabilizing stem–loop mutations diminishing loop stability. Utilizing a series of *pilE* translational fusions, deletion of either loop 1 or loop 2 caused a significant reduction of *pilE* mRNA resulting in reduced expression of the reporter gene. Consequently, the formation of the loops apparently protects the *pilE* transcript from degradation. Putative loop 3 contains the *pilE* ribosomal binding site. Consequently, its formation may influence translation. Analysis of a small RNA transcriptome revealed an antisense RNA being produced upstream of the *pilE* promoter that is predicted to hybridize across the 5′ untranslated region loops. Insertional mutants were created where the antisense RNA is not transcribed. In these mutants, *pilE* transcript levels are greatly diminished, with any residual message apparently not being translated. Complementation of these insertion mutants *in trans* with the antisense RNA gene facilitates *pilE* translation yielding a pilus + phenotype. Overall, this study demonstrates a complex relationship between loop-dependent transcript protection and antisense RNA in modulating *pilE* expression levels.

INTRODUCTION

Neisseria gonorrhoeae causes the sexually transmitted disease gonorrhea where the expression of pili on the cell surface has been shown to be crucial for infectivity (Kellogg *et al.*, 1968; Swanson, 1973; Swanson *et al.*, 1987). The pilus organelle consists of several proteins, with *PilE* polypeptide (encoded by the *pilE* gene) being the major component. Despite the importance of pili to the disease process, very little is known with regard to the regulation of expression of PilE polypeptide. The *pilE* promoter structure is complicated with three fully functional sense promoters being present (designated P1, P2 and P3), yet only the P1 promoter (sigma^{70} dependent) is used in the gonococcus (Fyfe *et al.*, 1995; Carrick *et al.*, 1997). In addition, two *pilE* antisense promoters have been identified: one located within a midgene region and the second one located at the 3′ end of the gene (Masters *et al.*, 2016). Despite considerable effort having been expended on trying to identify regulatory proteins, only one transcriptional cofactor has been found in the form of the small DNA-binding protein, integration host factor (IHF). When IHF binds upstream of the *pilE* promoter, IHF binding facilitates the interaction of two specialized AT-rich promoter sequences (UP elements) with RNA polymerase that increases transcription approximately 10-fold (Hill *et al.*, 1997; Fyfe & Davies, 1998).

mRNA turnover is believed to initiate in regions that are relatively free of bound ribosomes as their constant occupation on transcripts could enhance mRNA stabilization (Bechhofer & Dubnau, 1987). Consequently, 5′ and 3′ untranslated regions (UTRs) are considered to be good candidates as initial cleavage sites for RNases, with the formation of RNA secondary structures within these regions possibly influencing stability and/or translational efficiency (Régnier & Arraiano, 2000; Marzi *et al.*, 2008). Loop structures are predicted in the *Escherichia coli rpsT* P1 mRNA and analysis has shown that the presence of a hairpin at the 5′ end of the *rpsT* P1 transcript hinders both the pyrophosphohydrolase activity of RppH and the single-stranded-dependent cleavage of RNase E, thus prolonging mRNA half-life (Deana *et al.*, 2008). Consequently, the presence of

Abbreviations: DUS, DNA uptake sequence; IHF, integration host factor; qRT-PCR, quantitative real-time PCR; rbs, ribosomal binding site; sRNA, small antisense RNA; UTR, untranslated region.

One supplementary figure is available with the online Supplementary Material.

any *pilE* mRNA secondary structural features may also moderate transcript turnover.

The presence of naturally occurring small antisense RNAs (sRNAs) has been widely reported (Georg & Hess, 2011). However, the regulatory functions of many of these RNAs are still yet to be determined (Waters & Storz, 2009). Most of the known sRNAs do not encode protein, with their pervasive transcription being initiated from intergenic or intragenic promoters (Wade & Grainger, 2014). A recent analysis of a gonococcal small RNA transcriptome revealed many such sRNAs (Wachter & Hill, 2015). Such *trans*-encoded sRNAs appear to act primarily by regulating mRNA translation/degradation via complementary binding in an antisense manner that often requires the aid of Hfq protein, which is an RNA chaperone. The absence of Hfq protein causes pleiotropic effects that occasionally involve bacterial pathogenicity (Hoe *et al.*, 2013). Hfq also serves as a major post-transcriptional regulator of numerous stress-responsive genes (Sittka *et al.*, 2007). In a gonococcal *hfq* mutant, the absence of Hfq protein has been shown to decrease *pilE* transcript levels, as well as to influence several pilus-associated phenotypes (Dietrich *et al.*, 2009). In a *Neisseria meningitidis hfq* mutant, PilE polypeptide is absent (Pannekoek *et al.*, 2009). Consequently, these observations suggest that a small RNA may be involved in moderating *pilE* expression.

In this study, post-transcriptional effects on *pilE* expression were investigated and a stabilizing role for stem–loop structures in the 5′ UTR of the *pilE* message was indicated. Furthermore, as one loop structure is predicted to occlude the *pilE* ribosomal binding site, evidence is presented whereby an sRNA is required for translation of the *pilE* message. Overall, the data indicate that *pilE* expression is regulated at the post-transcriptional level adding a further layer of complexity to the regulation of this important virulence determinant.

METHODS

Strains and growth conditions. *N. gonorrhoeae* strain MS11 (Rocky Mountain Laboratories, Hamilton, MT, USA) was used in this study. Gonococci were passaged daily on a gonococcal typing medium (Swanson, 1982) at 37 °C in a 5 % CO_2 atmosphere. When grown in the presence of antibiotics, the final concentrations were as follows: chloramphenicol, 10 μg ml^{-1}; kanamycin, 80 μg ml^{-1}; erythromycin, 5 μg ml^{-1}.

E. coli cells were grown using LB medium at 37 °C. When *E. coli* carried recombinants, the medium was supplemented with antibiotics at the following concentrations: carbenicillin, 100 μg ml^{-1}; erythromycin, 200 μg ml^{-1}; chloramphenicol, 20 μg ml^{-1}; tetracycline, 15 μg ml^{-1}; and kanamycin, 40 μg ml^{-1}.

Construction of translational fusions. *pilE* translational fusions were constructed by fusing the *pilE* 5′ UTR (which included DNA comprising the first 19 codons) in-frame to a reporter gene, either beta-galactosidase (*lacZ*) or chloramphenicol acetyl transferase (*cat*), that lacked their cognate ribosomal binding site (rbs). This procedure entailed amplifying *pilE* with the appropriate set of primers (Table 1) and initially cloning the fragment into the pCRII (Invitrogen) vector. For construction of the WT_{pilE}*:lacZ* clone, the appropriate fragment was cut by *Eco*RI and *Bam*HI enzymes and ligated in the vector pRS414 that carries a truncated *lacZ* gene preceded by a strong transcriptional terminator, resulting pRS414-WT_{pilE}:*lacZ*(pTL2) vector. To create the loop 1 :: *lacZ* and the loop 2 :: *lacZ* deletion fusions, sequential PCR was employed that amplified the flanking regions to each loop followed by ligation of the fragments. The fragment containing the loop deletion was then cloned into vector pRS414 at the unique sites *Eco*RI and *Bam*HI to produce pRS414-L1del : *lacZ* (pTL6) and pRS414-L2del : *lacZ* (pTL8) constructs.

A similar approach was used to make *pilE : cat* translational fusions. The promoter-less *cat* gene was obtained from pCR2.1-*cat*:DUS (S. A. Hill, unpublished). Various *pilE* fragments containing intact or the 5′ UTR loop deletions were amplified using the appropriate primers (Table 1), followed by cloning into the pCRII vector; a double *Sac*I and *Sau*3AI digest released the fragment that was then inserted in the pCRII-*cat* vector. This protocol allowed us to generate pCRII-WT_{pilE}: *cat* (pTL14), pCRII-L1del : *cat* (pTL15) and pCRII-L2del : *cat* (pTL16) constructs.

In order to introduce the *pilE* :: *cat* translational fusions into the gonococcal chromosome, the various *pilE : cat* fusions were cloned into a pBluescript-*opaE:erm* vector that carries the *opaE* gene with an *ermC* gene inserted in the unique *Sal*I site. The fusions were then PCR amplified and inserted in pBluescript-*opaE:erm* at the unique *Xba*I site to create pBluescript-*opaE* :: *erm : pilE* :: *cat* constructs. These DNAs were then used to cross the fusions into the gonococcal *opaE* locus with transformants being selected through erythromycin resistance.

To investigate the effect of *pilE* antisense transcription on regulation of *pilE* across the 5′ loops, a kanamycin gene insertion was introduced into the *pilE* gene such that transcription of antisense RNAs across the loop structures would be disrupted. The *pilE* :: *kan* construct was generated by blunt-end ligation of the *kan* gene into the *pilE Bss*HII site. The appropriate orientation of the *kan* insert was confirmed by PCR to ensure interruption of antisense transcription. The pUC8-*pilE : kan* plasmid DNA was then used to transform the *N. gonorrhoeae* MS11 carrying a *pilE* :: *cat* translational fusion to kanamycin resistance to create a GC *pilE* :: *kan opaE* :: *erm : pilE* :: *cat* strain.

Site-directed mutagenesis was performed as previously described (Wachter *et al.*, 2015; Masters *et al.*, 2016).

Construction and complementation of the asRNA7 *ermC* insertion knockout mutants. Regions upstream of the *pilE* 5′ UTR in *N. gonorrhoeae* MS11 were disrupted with *ermC* insertions that were made by sequential ligation of PCR-generated DNA fragments and an *ermC* gene cassette. DNA transformation was then used to make the gonococcal mutants. The resulting constructs (ΔasRNA7 : *ermC*1-6) were then tested for transcription of full-length *pilE* message through Northern blot and endpoint reverse transcriptase PCR analysis. To determine the translational efficiency of these insertion mutants, a *cat* gene was translationally fused to the 3′ end of *pilE* and assessed the chloramphenicol resistance and competency.

To construct a ΔasRNA7 : *ermC* complement, the genomic region encoding a small RNA upstream of the *pilE* 5′ UTR corresponding to ΔasRNA7 : *ermC*5 and ΔasRNA7 : *ermC*6 was amplified with primers 10605 (5′-CCGTATGTTAACGCGTAAATTCAAAAATC-3′) and 09449 (5′-GCAACAAAAAACCGATGGTTAAATACATTGC-3′) and ligated to a *kan* gene cassette containing a gonococcal DNA uptake sequence (DUS) in a TA cloning vector. For subsequent transformation into *N. gonorrhoeae*, the *kan*:DUS : asRNA7 construct was ligated into the *opaE* gene within a pBlueScript cloning vector. The pBlueScript-*opaE : kan* : DUS : asRNA7 construct was then crossed into the *opaE* locus of *N. gonorrhoeae* strain MS11. Chromosomal DNA from the ΔasRNA7 : *ermC*6 mutational constructs was then used to transform the *opaE : kan* : DUS : asRNA7 cells, generating mutants ΔasRNA7 : *ermC6 : opaE* : asRNA7 : *kan*1, ΔasRNA7 : *ermC6 : opaE* : asRNA7 : *kan*2 and ΔasRNA7 : *ermC6 : opaE* : asRNA7 : *kan*3. Translational efficiencies of WT, ΔasRNA7 : *ermC*5 and ΔasRNA7 : *ermC*6 were determined through transformation efficiency and phenotypic assays.

Table 1. Primers used to make translational fusions

Primer	Sequence	Application
Fusion 1-*Hind*III	5′-CCCAAGCTTCCGAAGCCATCCTTTTGGCCGAA-3′	5′ UTR-PCR
Fusion 2	5′-TCAGCCGTTGCCGGGTATTG-3′	5′ UTR-PCR
Fusion 3-*Bam*HI	5′-ATAGCGATCAGAATCATCAGCTCGATAAGGG-3′	5′ UTR-PCR
L1-L-KpnI	5′-AAAAAGGTACCGACAACTGCGTATTATAAAGCAAG ATTCGTGCC-3′	Loop 1 deletion
L1-R-KpnI	5′- AAAAAGGTACCATGATGCCGATGGCGTAAGCC-3′	Loop 1 deletion
*Eco*RV–pRS	5′-CAGCAGGATATCCTGCACCATCGT-3′	Loop 1 deletion
L2-L-KpnI	5′-AAAAAAGGTACCATGCAATGTATTTAACCATCGGTTTTTTGTTGCG-3′	Loop 2 deletion
L2-R-KpnI	5′-AAAAAGGTACCTCCCCTTTCAATTAGGAGTAATTTTATGAATACCCTTCA-3′	Loop 2 deletion
Fusion 4	5′-TCGATTTCTTTGCCGTCTTTGG-3′	Loop 2 deletion
cat3-*Bam*HI	5′-AAGGATCCTGGAGAAAAAAATCACTGGATATA-3′	*cat* gene PCR
MM13R	5′-GTAAAACGACGGCCAGTGAATTGTA-3′	*cat gene PCR*
Fusion 5	5′-AAACGGGAAGTAGGCTCCCATGAT-3′	*pilE*::*lacZ fusions PCR*

RNA analysis. The conditions employed for RNA extraction, quantitative real-time PCR (qRT-PCR) analysis and primer extension analysis were as described previously (Wachter *et al.*, 2015; Masters *et al.*, 2016). The primer pairs used for loop analysis and translational fusion analysis are found in Table 2; primer pairs for the assessment of the gonococcal insertion mutants have been previously described (Wachter *et al.*, 2015).

Loop formation assay. The assay was utilized to determine whether the 5′ UTR stem–loops are formed under non-denaturing *in vitro* conditions using qRT-PCR analysis. *E. coli* carrying the *pilE*-containing vector pVD203 was grown to the exponential phase (OD_{600} reaching 0.5) at which point *pilE* mRNAs were extracted. *pilE*-specific, reverse-transcribed cDNAs were then subjected to qRT-PCR reactions utilizing the forward primers that were designed such that each primer resided within each predicted loop sequence. The reverse primers were designed such that they recognized nucleic acid sequences outside of the loop structures and that the amplified products that were produced were of a similar size, 160 bp. If the stem–loop structures are formed due to base pairing following RNA purification under native conditions, then PCRs using the primers within each loop should produce little or no products as base-paired loop sequences are not available for hybridization with the primers. In control experiments, the addition of betaine (a denaturing agent) in the qRT-PCR mix was employed to disrupt loop formation during the qRT-PCR experiments.

Computer modeling analysis. Mfold (Zuker, 2003) and RNAstructure (Bellaousov *et al.*, 2013) web servers were used for analysis of RNA secondary structures within the 5′ UTR of *pilE*.

RESULTS

Protection of the *pilE* transcript through loop formation

When the IHF binding site, which is located immediately upstream of the *pilE* promoter, was deleted, transcription was diminished approximately 10-fold (Hill *et al.*, 1997; Fyfe & Davies, 1998). However, stable residual full-length *pilE* message is evident when total RNA is assessed by both Northern blotting and primer extension analysis (Hill *et al.*, 1997). However, this residual message does not appear to be translated (Fig. S1, available in the online Supplementary Material). Consequently, we explored the possibility that *pilE* mRNA structural elements may have contributed to the above-mentioned observations. *In silico* analysis of the 5′ UTR of the *pilE* message using the Mfold (Zuker, 2003) and RNA structure (Bellaousov *et al.*, 2013) applications

Table 2. Oligonucleotide primers used in qRT-PCR analysis involving 5′ UTR loops

Primer	Nucleotide sequence	Application
Loop 1	5′-TTGTCGCAACAAAAAACCGATGGTTAAA- 3′	Loop 1-forward
Loop 2	5′-AAAAAAGGTACCATGATGCCGATGGCGTAAGCC-3′	Loop 2-forward
Loop 3	5′-CCCTTTCAATTAGGAGTAATTTTATGAATACCCTTC-3′	Loop 3-forward
RC3	5′-GTCGGCATTTTGGCGGCAGTCG-3′	Outside the loops-forward
RC4	5′-GATAGCGATCAGAATCATCAGCTCGATAAGGG-3′	Loop 1-reverse
tsp5	5′-CCGTGTAGTCTTGGTAGGCGGGAA-3′	Loop 2-reverse
09173	5′-TTGACCTTCGGCCAAAAGGATGGCTTCGGAAAC-3′	Loop 3-reverse
tsp4	5′-CGCCGGCAGAAGTGTTGTTTTC-3′	Outside the loops-reverse
lacZ fusion 1	5′-GTCGGCATTTTGGCGGCAGTCG-3′	
lacZ fusion 2	5′-GCTTCTGGTGCCGGAAACCAGGC-3′	
cat fusion 1	5′-CACTGGATATACCACCGTTGATATATCCCAATCGCATCGTAAAGAACA-3′	
cat fusion 2	5′-GTGAACACTATCCCATATCACCAGCTCACCGTCTTTCATTGC-3′	

revealed the potential for three thermodynamically stable stem–loop structures to form (Fig. 1a). Consequently, transcript levels, and/or protein expression, may be a subject to post-transcriptional regulation by such *cis*-embedded elements, especially as one of the predicted loops (designated loop 3 or L3) contains the *pilE* rbs and the AUG start codon. When primer extension analysis was performed using *pilE* mRNA, several secondary premature 5′ endpoints were observed in addition to the prominent signal for the true transcriptional start site (Fig. 1b; arrows). These secondary 5′ endpoints mapped to AU-rich regions in the predicted loop 2 (Fig. 1a; arrows). The *pilE* gene of *N. gonorrhoeae* was reported to possess three promoter sequences (designated P1, P2 and P3), with the sigma^{70}-type P1 being the only active *pilE* promoter in GC (Fyfe *et al.*, 1995). None of the 5′ endpoints maps to the tsp of these alternative promoters. However, recent analysis of transcription within the *pil* system has revealed the existence of alternative promoter usage using non-cognate promoter elements (Wachter *et al.*, 2015). Whether alternative promoter usage

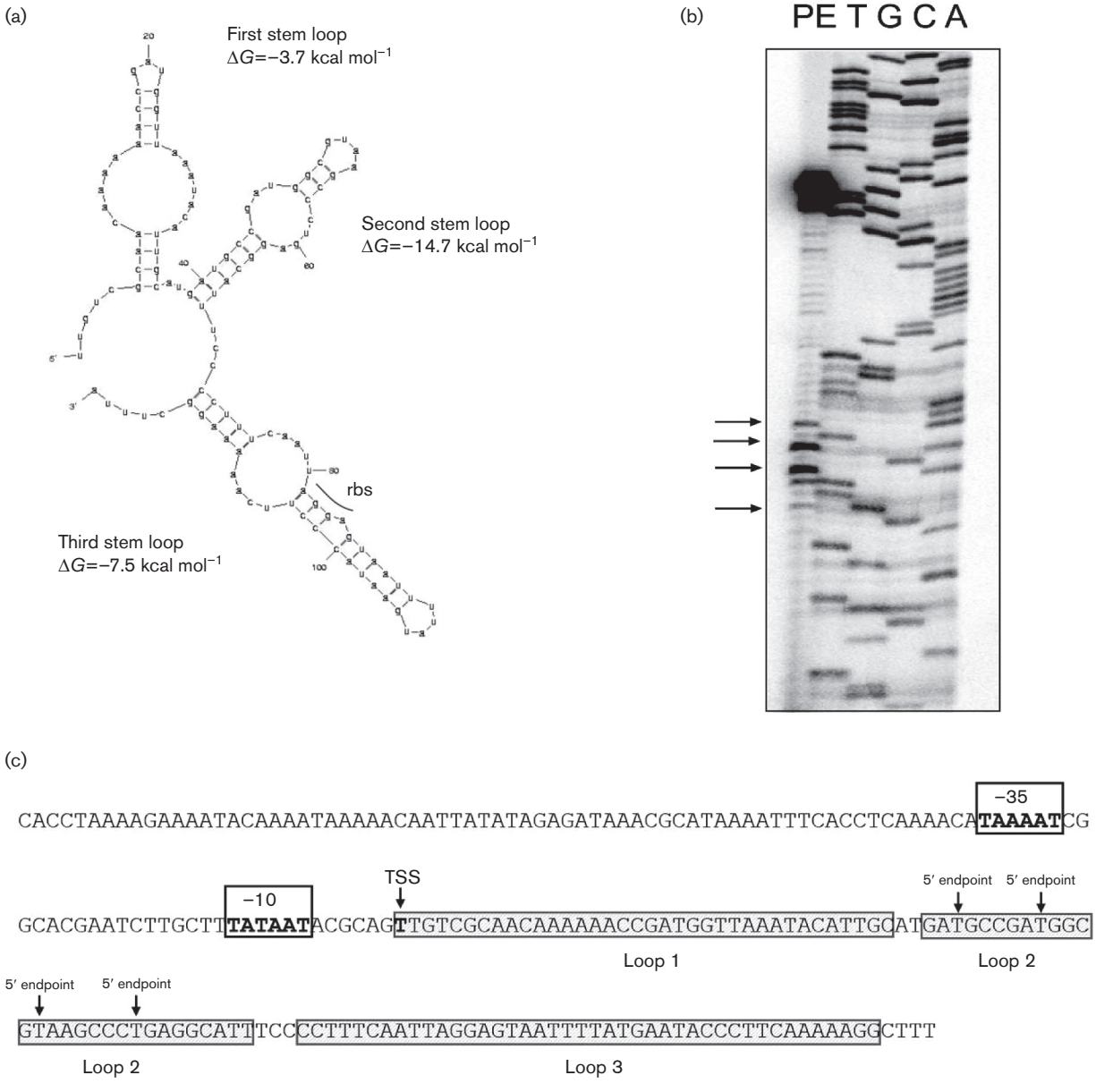

Fig. 1. RNA secondary structural analysis. (a) *pilE* mRNA was analysed using the Mfold algorithm that revealed three potential secondary structural features with highly favourable predicted free energy values within the 5′ UTR of *pilE*. The loops are designated loops 1, 2 and 3. The rbs is indicated in loop 3. (b) Primer extension analysis of *pilE* mRNA. The arrows in both panels (b) highlight potential alternative 5′ mRNA endpoints. (c) Schematic diagram indicating the location of the alternative 5′ mRNA endpoints.

accounts for the secondary 5′ endpoints has not been explored in the current manuscript. Consequently, the secondary 5′ endpoints mapped within the loop 2 of *pilE* mRNA may be products of either endonucleolytic cleavage or non-cognate promoter usage.

qRT-PCR was used to determine whether these putative *pilE*-specific RNA loop structures form. In these assays, primer pairs were designed such that the forward primer was located within each putative loop structure, with the reverse primer being located outside of the predicted loop structures. Primer design was such that the amplified products were similar in size (160 bp). Consequently, if base pairing occurred within the predicted loop structures, then it was hypothesized that the loop structures would be less accessible to the forward primer during the amplification process (Fig. 2a). *pilE* mRNA was prepared following transcription of the *pilE* gene carried on plasmid pVD203 (Bergström *et al.*, 1986); the qRT-PCR data presented in Fig. 2b indicate the formation of all three loop structures in the *pilE* 5′ UTR mRNA.

The formation of the *pilE* 5′ UTR stem–loops was further investigated through site-directed mutagenesis where the predicted loop sequences were changed such that RNA secondary structure would be disrupted. Mutagenic primers were designed for each loop that would impede complementary base pairing (Fig. 3a), with individual loop stability again being assessed by the qRT-PCR assay. When the loops were mutated, the forward primer was able to gain access to the RNA yielding a product (Fig. 3b), indicating that the previous negative observations were due to *pilE* 5′ UTR loop formation. The data are presented in a $\log_{10}$ scale of *pilE* expression compared to expression of the internal control *amp* gene carried on the plasmid. The higher the log value indicates more-amplified product and relates to the loops not forming. A similar qRT-PCR approach was also utilized to examine loop stability when the putative loops were individually deleted (Fig. 3c). Again, the presence of an amplified product indicates loop destabilization. For example, when loop 2 or 3 was deleted, the RNA became accessible to the loop 1 primer; when loops 1 and 3 were deleted, the RNA became accessible to the loop 2 primer; and when loop 1 was deleted, the RNA became accessible to the loop 3 primer. However, in contrast to these observations, when loop 2 was deleted, loop 3 is still able to form.

Overall, these combined experiments indicated that (i) the stem–loops form through complementary base pairing

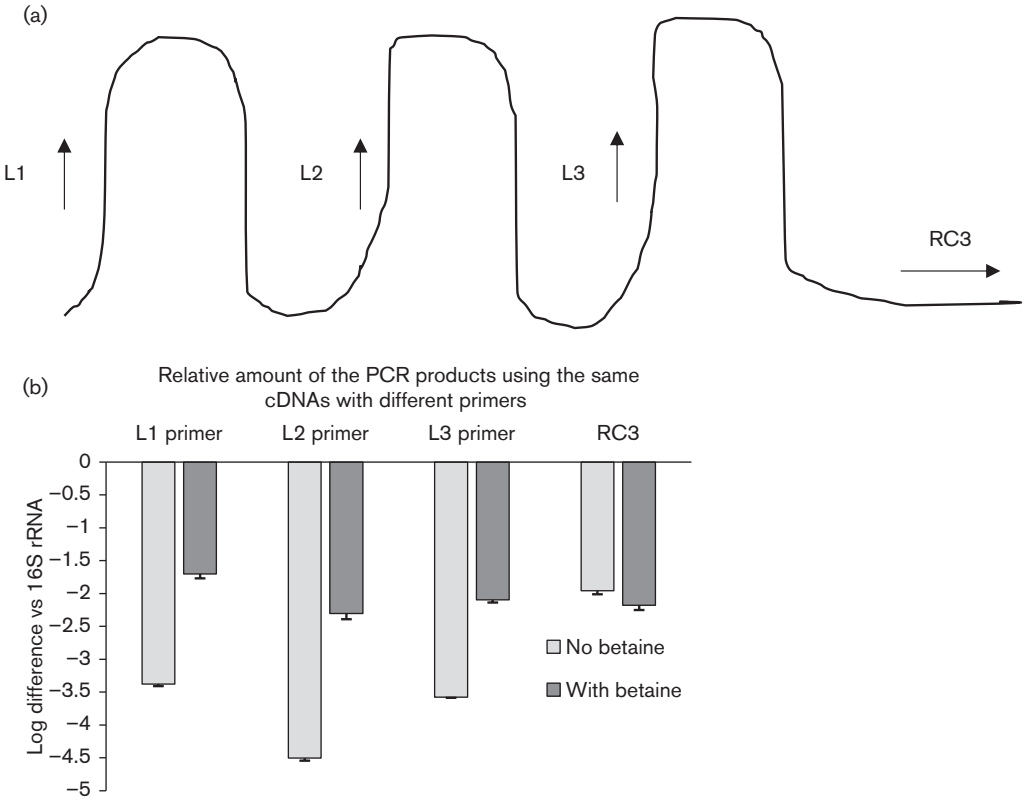

Fig. 2. Loop formation in *pilE* mRNA. (a) Schematic representation indicating the relative location of each forward primer. (b) qRT-PCR analysis indicating the relative amount of cDNA using the above-mentioned primers. When the loop primers were used in the qRT-PCR analysis, less-amplified products were observed when compared to the product from the primer located outside of the loop (RC3). The error bars reflect ±SD; n=3. L1 primer vs RC3, P<0.001; L2 primer vs RC3, P<0.001; L3 primer vs RC3, P<0.001.

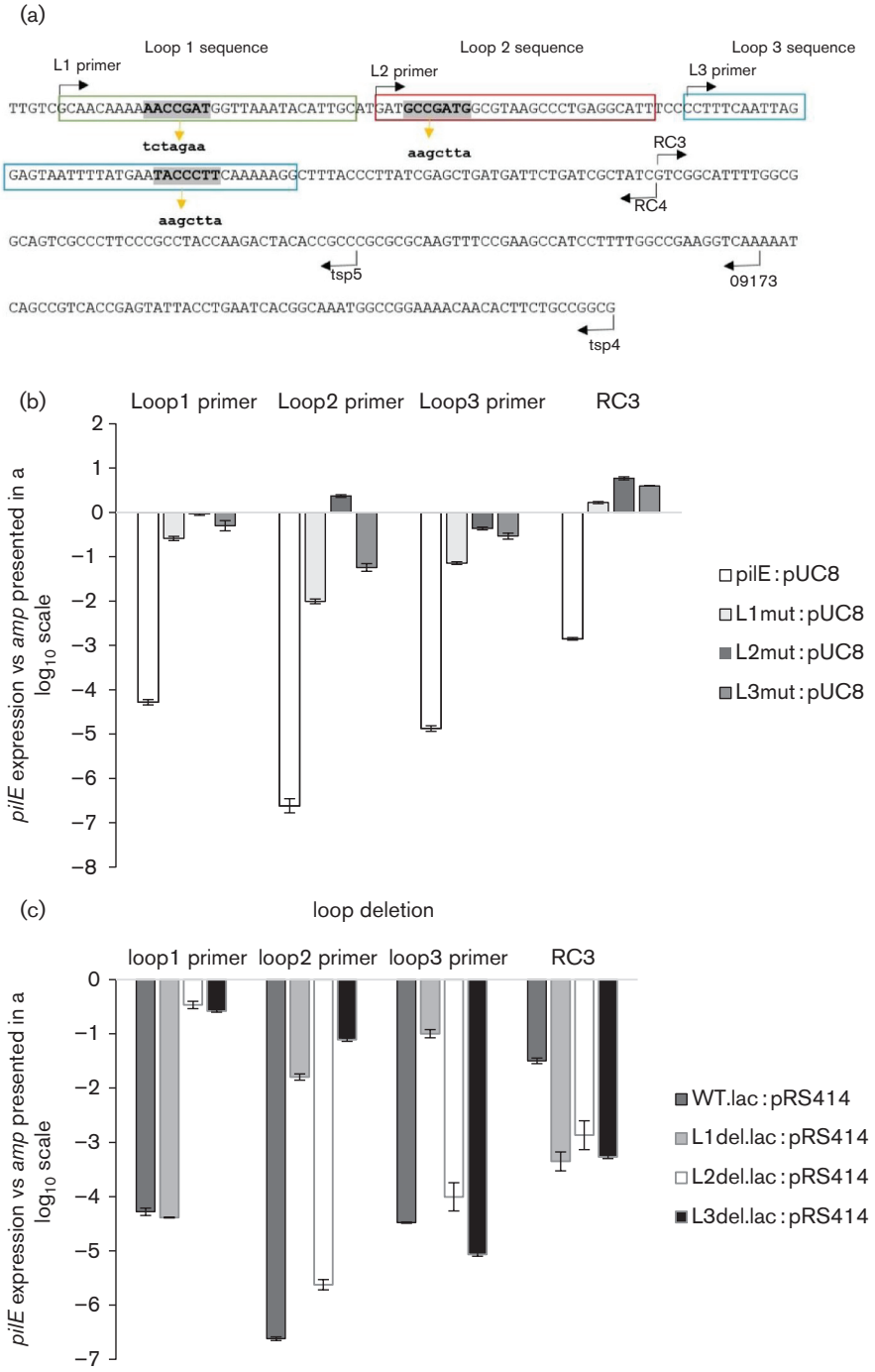

Fig. 3. Stability of the putative loop structures. (a) Nucleotide sequence of the 5′ UTR of *pilE* (in uppercase letters) and relative position of the primers used in qRT-PCRs; each putative loop sequences is boxed. The loop sequences (boldface uppercase letters) were mutated to alternative sequences (boldface lowercase letters below the sequence) that were predicted to disrupt loop formation. (b) qRT-PCR analysis using constructs containing nucleotide substitutions. (c) qRT-PCR analysis of loop deletion mutants. In (b) and (c), expression levels of *pilE* transcripts were calculated by subtracting expression of the internal control beta-lactamase gene carried on the plasmid. The error bars reflect ±SD; n=4. In (b), P values of the mutated constructs are compared to the non-mutated *pilE* construct: Loop 1 primer : L1mut, P<0.001; L2mut, P<0.001; L3mut, P<0.001 : Loop 2 primer : L1mut, P<0.001; L2mut, P<0.001; L3mut, P<0.001; Loop 3 primer: L1mut, P<0.001; L2mut, P<0.001; L3mut, P<0.001. In (c), P values of the mutated constructs are compared to the non-mutated *pilE* construct: Loop 1 primer: L1del, P<0.001; L2del, P=0.004; L3del, P=0.001; Loop 2 primer: L1del, P<0.001; L2del, P<0.001; L3del, P=0.001; Loop 3 primer: L1del, P<0.001; L2del, P<0.001; L3del, P<0.001.

within the *pilE* 5′ UTR (Fig. 2b), (ii) mutating an individual loop through site-directed mutagenesis also affects the formation/stability of the other loops (Fig. 3b) and (iii) individually deleting any of the loops also disrupts loop stability except for the one exception noted above (Fig. 3c).

The *pilE* 5′ UTR provides a protective role in maintaining *pilE* transcript levels

To determine what effect loop formation plays in *pilE* expression, we focused on the loop deletions and constructed a series of translational fusions, where loop 1 and loop 2 were individually deleted. The deleted *pilE* 5′ UTR segments were then fused in-frame to one of two truncated reporter genes, beta-galactosidase (*lacZ*), or, chloramphenicol acetyl transferase (*cat*), with each reporter gene lacking its own rbs. The deleted constructs were then compared to an equivalent WT construct; relative expression was measured by growth on solid medium, by qRT-PCR analysis and by biochemical analysis. qRT-PCRs were performed using RNAs that were isolated from the different constructs under the same conditions, thus reflecting their relative protective role. Since loop 3 contains the rbs that is needed for translation of the reporter gene, a loop 3 deletion mutant could only be used to determine relative RNA stability. The data presented in Fig. 4a show the growth of each beta-galactosidase fusion strain on solid medium containing the *lacZ* indicator X-Gal. The data presented in Fig. 4b assess the relative RNA levels by qRT-PCR analysis from the various *pilE*::*lacZ* fusions, with Fig. 4c showing the corresponding biochemical analysis. From these combined experiments, we conclude that when loop 1, loop 2 or loop 3 is individually deleted, there is a significant reduction in the amount of RNA compared to WT (for all three deletion constructs, $P<0.001$; $n=3$), which is also reflected at the protein level for loop 1 and loop 2 mutants ($P<0.001$; $n=15$). Moreover, because very little relative RNA is observed with the

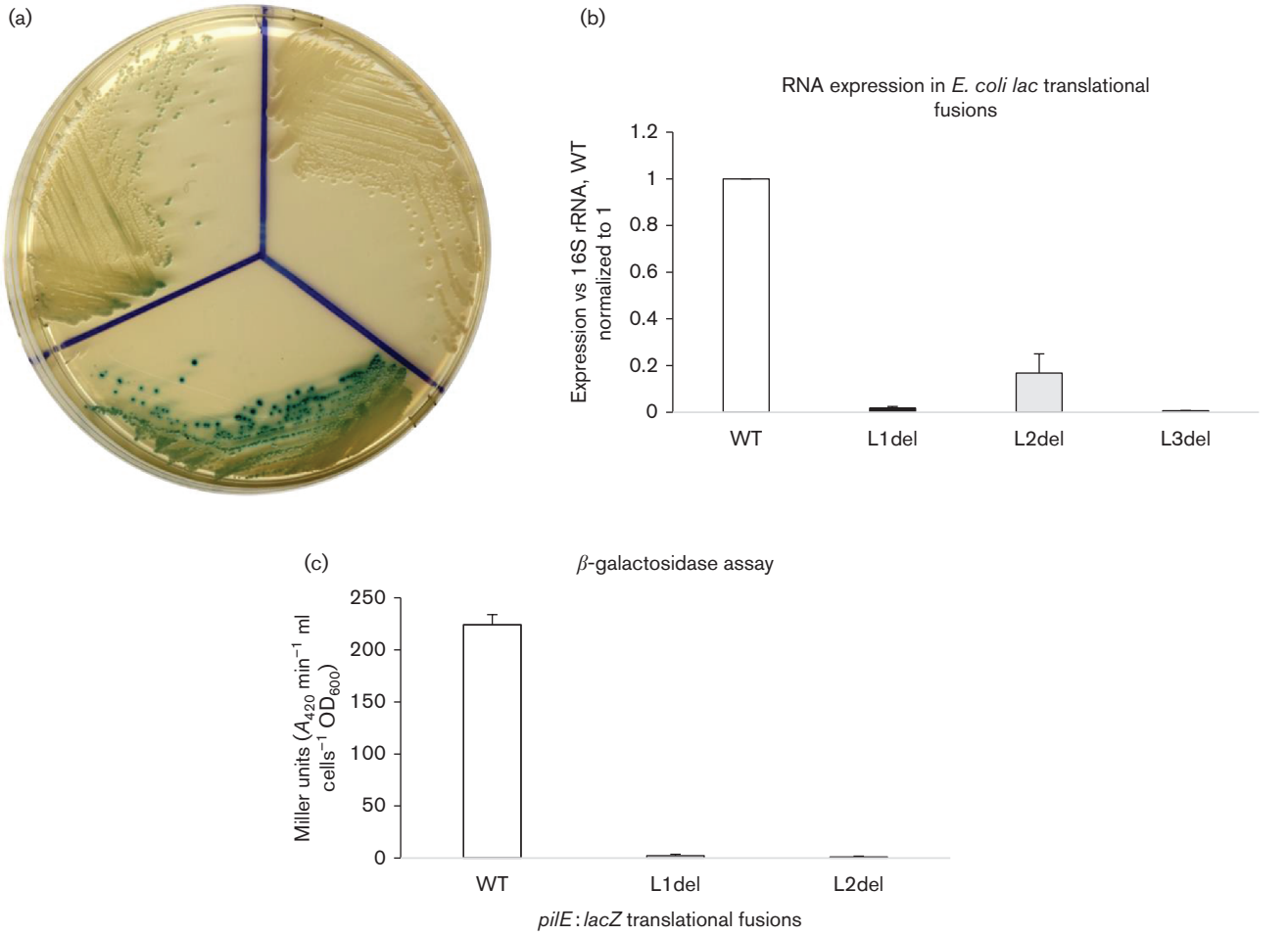

Fig. 4. *pilE* translational fusion analysis. The effects of the 5′ UTR loops on the expression of *pilE*::*lacZ* translational fusions in *E. coli*. (a) Growth of the different *pilE*::*lacZ* translational fusion strains (WT, loop 1 deletion and loop 2 deletion) on solid medium containing X-Gal. (b) qRT-PCR analysis of the various deletion strains compared to WT that is set at unity. Error bars reflect ±SD; $n=3$; L1del, $P<0.001$; L2del, $P<0.001$; and L3del, $P<0.001$. The expression levels were compared to a 16S RNA control. (c) Biochemical analysis of beta-galactosidase activity. The error bars reflect ±SD; $n=15$; when compared to WT, L1del ($P<0.001$) and L2del ($P<0.001$).

loop 2 deletion fusion (Fig. 4b) (even though loop 3 still forms; Fig. 3c), this implies that loop 1 is likely to be the critical loop structure for protection of the *pilE* message. Qualitatively similar results were also obtained from comparable *pilE* :: *cat* translational fusions where the individual loops were deleted, as well as in *lacZ* translational fusions where the formation of the loop structures was impaired through site-directed mutagenesis. Consequently, these data imply a protective role for the *pilE* 5′ UTR stem–loops.

Analysis of *pilE* :: *cat* translational fusions in gonococci

To determine whether the *pilE* 5′ UTR loops play a similar role in the gonococcus, *pilE*::*cat* translational fusions were placed ectopically on the gonococcal chromosome within the *opaE* locus. As each fusion construct contained the *pilE* leader peptide encoding sequence, only mRNA analysis could be performed as any protein product would be secreted from the cell. The data presented in Fig. 5a show the expression levels of the fused *cat* RNAs produced by the WT and loop deletion constructs. Consistent with the *E. coli* data, individual loop deletions caused a significant decrease in expression of the reporter gene at the RNA level when compared to WT ($P<0.001$ for both deletion fusions; $n=4$).

In the above-mentioned experiment, a WT copy of the *pilE* gene was also present within the cells (genotype *pilE*+ *opaE* :: *pilE* :: *cat*; Fig. 5b). Consequently, *pilE* antisense RNA that originates from the mid-gene intragenic promoter is also being produced within these cells. Consequently, this antisense RNA may bind across the 5′ UTR fusion loops (Masters *et al.*, 2016). When the resident *pilE* gene was mutated through a kanamycin gene insertion that blocks *pilE* antisense RNA production across the loops, a twofold to threefold increase in *cat* RNA level was observed (Fig. 5c; $P<0.001$; $n=4$). Consequently, this observation suggests that expression of *pilE cis*-antisense RNA may affect stem–loop formation by making the *pilE* transcript more susceptible to degradation.

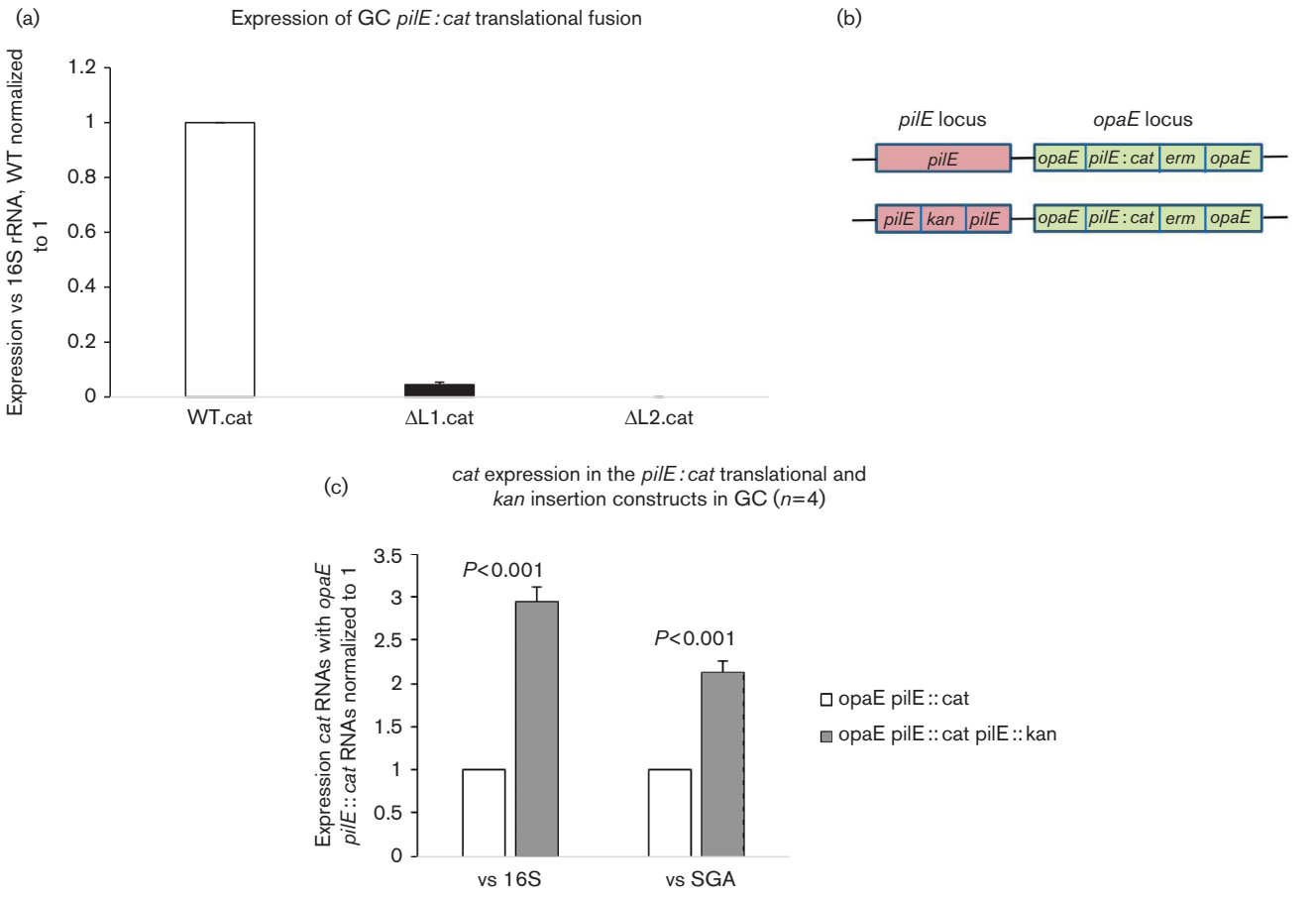

Fig. 5. *pilE* :: *cat* translational fusions in gonococci. (a) qRT-PCR analysis of the various deletion strains compared to WT that was set at unity. Expression levels were compared to a 16S RNA control. The error bars reflect ±SD; $n=6$; when compared to WT, L1del.cat ($P=0.042$) and L2del.cat ($P<0.001$). (b) Schematic representation of the two gonococcal constructs. It shows where the insertion mutations are located on the chromosome at the *pilE* and *opaE* loci. The insertion of the kanamycin gene prevents antisense transcription across the loop regions of the *pilE* from the intragenic promoters. (c) qRT-PCR analysis of the *pilE*::*cat* expression in these constructs. The *opaE* :: *pilE* :: *cat* is normalized to unity. The error bars reflect ±SD; $n=4$.

sRNA predicted to bind to the 5′ UTR of the *pilE* transcript

In many systems, *trans* regulatory elements are often found adjacent to the gene in question. Therefore, to test this possibility that a regulatory element resides upstream of the *pilE* promoter, gonococcal strains were constructed such that non-homologous gene inserts encoding erythromycin resistance were placed at regular intervals (six insertional mutants were constructed) upstream of the IHF binding site; a chloramphenicol acetyl transferase (*cat*) gene lacking its cognate rbs was also fused in-frame downstream of the *pilE* gene (Fig. 6a). RNA was then isolated from each mutant and *pilE* mRNA production was assessed by Northern blotting. From the blots presented in Fig. 6b, *pilE* transcription is apparent in all strains except for the two insertion mutants that are closest to the IHF binding site (oligonucleotide 245; insertions 5 and 6; 63 bp and 18 bp upstream of the IHF binding site; respectively). When an *ermC* gene cassette was placed 89 bp upstream of the IHF binding site (insert 4), *pilE* mRNA was observed. The production of *pilS*-derived sRNA (oligonucleotide 246) did not appear to be affected (Wachter *et al.*, 2015). However, with the use of the more sensitive endpoint PCR amplifying reverse-transcribed cDNAs (real-time PCR assay), *pilE* message was still apparent in mutants 5 and 6. This result suggests that the *pilE* RNA is still being transcribed in the insertion mutants 5 and 6, albeit less efficiently when compared to transcription from the other strains, yielding less *pilE* transcript in the mutants 5 and 6. The difference between the observations with real-time PCR analysis and the Northern blot analysis is likely due to the sensitivity of the two assays. However, the translational efficiency of cells containing these inserts was greatly reduced as these cells displayed neither chloramphenicol resistance nor competence as the cells were non-piliated (Fig. 6c). Competence is measured by the ability of the bacteria to take up exogenous *Neisseria*-specific DNA via

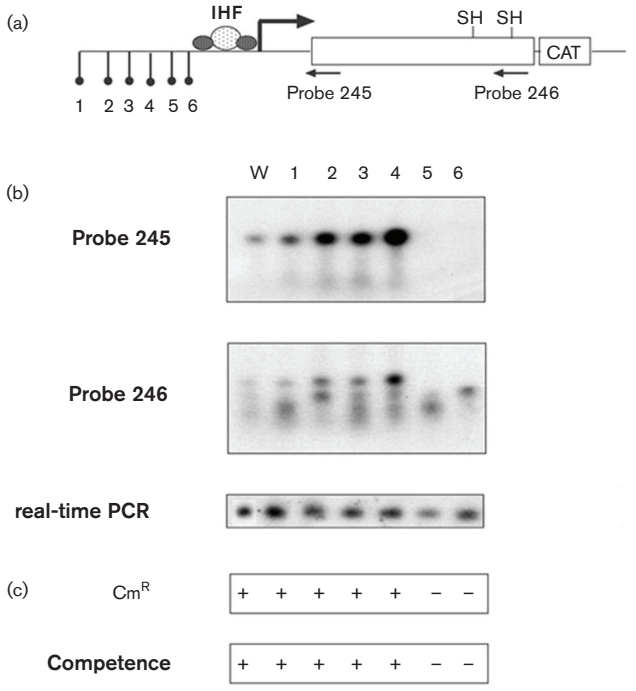

Fig. 6. Effect of upstream insertions on *pilE* transcription and translation. (a) Schematic representation of the *pilE* gene showing the relative positions of the *ermC* insertions and *cat* translational fusion. Distance of insertions from the *pilE* IHF binding site: 1, 562 bp; 2, 277 bp; 3, 162 bp; 4, 89 bp; 5, 63 bp; 6, 18 bp. (b) Transcriptional analysis of *pilE* with Northern blot utilizing a *pilE*-specific and *pilS*-specific probes (probes 245 and 246, respectively; Wachter *et al.*, 2015) and endpoint PCR using *pilE* reversed-transcribed cDNA templates (real-time PCR) of WT and the *ermC* insertion cells. (c) Translational analysis as determined by resistance of the gonococcal mutants to chloramphenicol (10 μg m^{-1}) and competence for DNA transformation (a positive score reflects a transformation efficiency of approximately 1×10^{-3} transformants per millilitre per microgram DNA; a negative score reflects a transformation efficiency of $<1\times10^{-8}$ transformants per millilitre per microgram DNA).

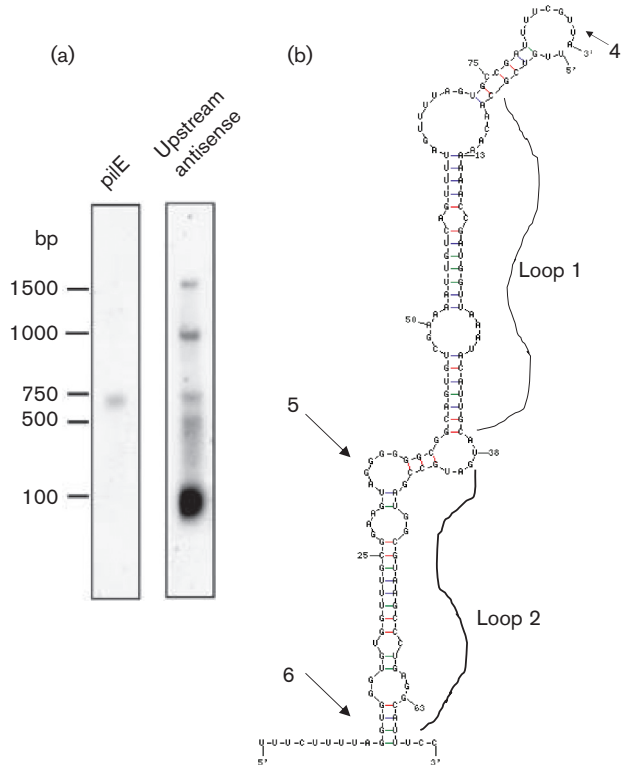

Fig. 7. Analysis of asRNA7. (a) Northern blot analysis of total RNA isolated from *N. gonorrhoeae.* The left panel is probed with a *pilE*-specific probe 245 (Wachter *et al.*, 2015); the right panel is probed with an oligonucleotide designed to bind to asRNA7. (b) Predicted interactions of asRNA7 and *pilE* 5′ UTR mRNA. asRNA7 has the potential to bind the 5′ UTR of *pilE* and expose the ribosomal binding site. The sites of the *ermC* insertions 4, 5 and 6 are indicated by arrows on the figure. This predicted interaction would be energetically favourable, with a $\Delta G=-28.7$ kcal mol^{-1}.

DNA transformation and is tightly linked to the piliation status of the organism as mutations causing loss of pilus expression lead to transformation incompetence; in this study, a negative competence score reflected a transformation frequency of $<1\times10^{-8}$ transformants per millilitre per microgram of DNA in contrast to a positive competence score of at least 1×10^{-3} transformants per millilitre per microgram of DNA (Koomey *et al.*, 1991; Tønjum & Koomey, 1997). Therefore, given the above-mentioned observations, we further explored whether a regulatory element resided between inserts 4 and 6.

The previously described *N. gonorrhoeae* small RNA transcriptome (Wachter & Hill, 2015) was assessed for potential sRNA molecules within this region and a single sRNA (designated asRNA7) was found. An oligonucleotide probe was designed to recognize this antisense sRNA species, and a strong signal was observed at approximately 100 bp on a Northern blot (Fig. 7a). *In silico* hybridization analysis was then performed between the putative asRNA7 and the 5′ UTR of the *pilE* transcript, with complementary binding being predicted with a favourable free energy ($\triangle G=-28.3$ kcal mol^{-1}) (Fig. 7b). Therefore, if asRNA7 binds to the 5′ UTR of the *pilE* transcript, such binding could potentially denature the secondary loop structures and expose the ribosomal binding site, thus allowing for translation. Complementation of insertion mutants 5 and 6 with the asRNA7 gene placed within the *opaE* locus (*opaE* :*kan*:DUS:asRNA7) caused the cells to become piliated, regain competence and express WT levels of *pilE* mRNA (Fig. 8). Consequently, asRNA7 apparently stabilizes the *pilE* transcript in readiness for translation.

DISCUSSION

The impetus for the current study was the *in silico* identification of three putative stem–loop structures in the 5′ UTR of the *pilE* transcript. The loops were shown to form in *pilE* mRNA (Fig. 2) and disruption of these sequences, either by site-directed mutagenesis or by individually removing the loop sequences, destabilized loop stability causing the mRNA to be more susceptible to degradation (Figs 3, 4 and 5). Consequently, the 5′ UTR loops appear to be able to protect *pilE* mRNA from degradation. Similar observations have been made where loop structures within the 5′ UTR of the *ompA*, *rne* and *cspE* mRNA in *E. coli* (Arnold *et al.*, 1998; Uppal *et al.*, 2008; Schuck *et al.*, 2009), as well as within the 5′ UTR of the *ermC* mRNA in *Bacillus subtilis* (Bechhofer & Dubnau, 1987), protect the mRNA, as in each case the presence of a loop prolonged mRNA half-lives. How the *pilE* loop structures protect the RNA is currently under investigation.

Loop structures in a 5′ UTR can determine the fate of transcripts not only by controlling stability but also by influencing translational efficiency (Régnier & Arraiano, 2000; Marzi *et al.*, 2008). The presence of RNA secondary structures in the *pilE* 5′ UTR region may explain why residual *pilE* mRNA remained when the IHF binding site located upstream of the *pilE* promoter was deleted (Hill *et al.*, 1997). However, what was not evident in that study was why this residual mRNA was not translated into PilE polypeptide (Fig. S1). A possible explanation for the lack of translation is that in the construction of the *pilE* IHF deletion mutants, not only was the IHF binding site deleted but also other upstream DNA was removed, causing the asRNA7 gene to be absent as well (Hill *et al.*, 1997). Consequently, without asRNA7, the loop structures would remain, with the *pilE* ribosome binding site still

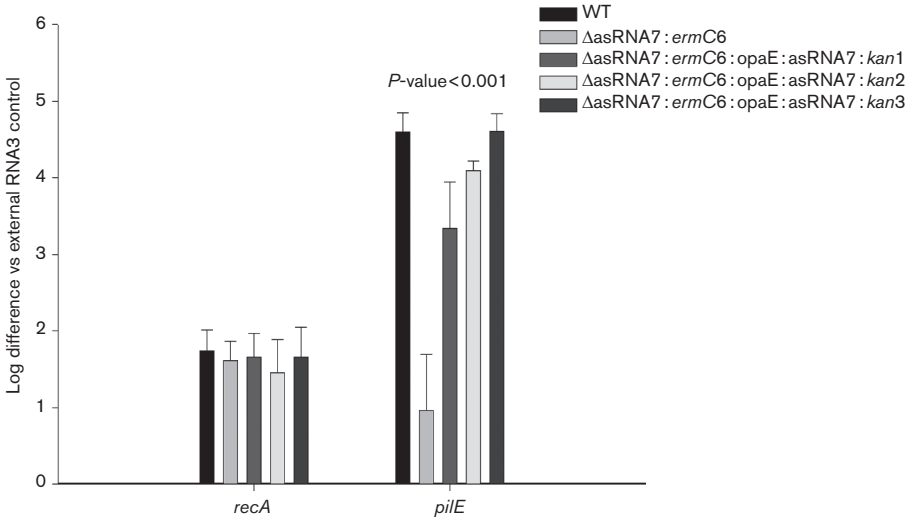

Fig. 8. qRT-PCR analysis of asRNA7 constructs. qRT-PCR analysis of WT, asRNA7 insertion mutant 6 (ΔasRNA7 : *ermC*6) and asRNA7 complements 1, 2 and 3 (ΔasRNA7 : *ermC6:opaE* : asRNA7 : *kan*1, 2 and 3) utilizing primer pairs specific for *recA* and the 5′ end of *pilE* (Masters *et al.*, 2016). The relative log difference as compared to an external RNA3 control. The error bars reflect ±SD; $n=6$; $P<0.001$.

being occluded, thus preventing translation. Likewise, with the insertion mutants 5 and 6, where asRNA7 antisense RNA is also absent, *pilE* mRNA in each of these mutants is unstable with any residual *pilE* transcripts also apparently not being translated (Figs 6 and 8). Interestingly, the insertions at the positions 2, 3 and 4 appear to stimulate *pilE* transcription (Fig. 6b, probe 245). Since these locations are within the vicinity of the *pilE*-specific, G4-associated asRNA and its promoter region (Cahoon & Seifert, 2013), it could be that these insertions negate any *cis*-mediated effects caused by G4 asRNA transcription that, in turn, enhances production of the asRNA7 from its promoter resulting in an increase in stabilization of the *pilE* primary transcript in these mutants. When the asRNA7 gene complements insertion mutants 5 and 6, *pilE* mRNA is again observed and is translated yielding a pilus + phenotype. Therefore, as the asRNA7 antisense RNA is predicted to bind to the *pilE* 5′ UTR across loops 1 and 2, it would appear that asRNA7 serves as a small RNA that facilitates mRNA protection, and, after binding, loop 3 presumably opens allowing access to the previously occluded ribosome binding site. Consequently, the *pilE* transcript could now be translated into PilE polypeptide. A slightly similar scenario has recently been presented regarding an operon involved in Type IV DNA secretion in the gonococcus. In this study, an RNA switch mechanism that involves two putative stem–loop structures contained within the 5′ UTR of the secretion operon has been proposed, one of which occludes the rbs within a putative loop structure; this occluded rbs is then released under certain conditions thus allowing for translation (Ramsey *et al.*, 2015).

In a previous study, it was demonstrated that there exists an inverse relationship between the level of *pilE* sense RNA levels and antisense RNA production across the *pilE* gene (Masters *et al.*, 2016). Consequently, a titration model was proposed whereby the presence of *pilE* antisense transcription helped determine the amount of *pilE* sense transcript levels. In the analysis of the *cat* translational fusions in the gonococcus (Fig. 5), elimination of *pilE*-specific antisense RNA derived from the midgene antisense promoter allowed twofold to threefold more message to be observed, suggesting that *pilE* antisense transcription may either impede loop formation in the 5′ UTR or alternatively compete with asRNA7 for binding to loops 1 and 2. Therefore, it would seem that there needs to be an orchestrated coordination of antisense RNA production across the *pilE* locus (both within the *pilE* gene and upstream with transcription of the asRNA7 gene) in order to obtain optimal transcript levels and to maintain appropriate PilE polypeptide levels. Whether this is achieved by differential promoter strengths, coordinated IHF binding or varying supercoiling fluxes across the *pilE* locus is currently unknown. Regardless, what has become apparent in this study is that, for a gene where no apparent regulatory protein has been identified, a complex regulatory circuit exists to maintain transcript levels operating in conjunction with a sophisticated translational scheme in order to optimize production of this important virulence determinant in the gonococcus.

ACKNOWLEDGEMENT

This study was supported by National Institutes of Health grant 1R15 AI072720-01A1 to S. A. H.

REFERENCES

Arnold, T. E., Yu, J. & Belasco, J. G. (1998). mRNA stabilization by the ompA 5′ untranslated region: two protective elements hinder distinct pathways for mRNA degradation. *RNA* **4**, 319–330.

Bechhofer, D. H. & Dubnau, D. (1987). Induced mRNA stability in *Bacillus subtilis*. *Proc Natl Acad Sci U S A* **84**, 498–502.

Bellaousov, S., Reuter, J. S., Seetin, M. G. & Mathews, D. H. (2013). RNAstructure: web servers for RNA secondary structure prediction and analysis. *Nucleic Acids Res* **41**, W471–W474.

Bergström, S., Robbins, K., Koomey, J. M. & Swanson, J. (1986). Piliation control mechanisms in *Neisseria gonorrhoeae*. *Proc Natl Acad Sci U S A* **83**, 3890–3894.

Cahoon, L. A. & Seifert, H. S. (2013). Transcription of a *cis*-acting, noncoding, small RNA is required for pilin antigenic variation in *Neisseria gonorrhoeae*. *PLoS Pathog* **9**, e1003074.

Carrick, C. S., Fyfe, J. A. & Davies, J. K. (1997). The normally silent sigma54 promoters upstream of the *pilE* genes of both *Neisseria gonorrhoeae* and *Neisseria meningitidis* are functional when transferred to *Pseudomonas aeruginosa*. *Gene* **198**, 89–97.

Deana, A., Celesnik, H. & Belasco, J. G. (2008). The bacterial enzyme RppH triggers messenger RNA degradation by 5′ pyrophosphate removal. *Nature* **451**, 355–359.

Dietrich, M., Munke, R., Gottschald, M., Ziska, E., Boettcher, J. P., Mollenkopf, H. & Friedrich, A. (2009). The effect of *hfq* on global gene expression and virulence in *Neisseria gonorrhoeae*. *FEBS J* **276**, 5507–5520.

Fyfe, J. A., Carrick, C. S. & Davies, J. K. (1995). The *pilE* gene of *Neisseria gonorrhoeae* MS11 is transcribed from a sigma 70 promoter during growth *in vitro*. *J Bacteriol* **177**, 3781–3787.

Fyfe, J. A. & Davies, J. K. (1998). An AT-rich tract containing an integration host factor-binding domain and two UP-like elements enhances transcription from the pilEp1 promoter of *Neisseria gonorrhoeae*. *J Bacteriol* **180**, 2152–2159.

Georg, J. & Hess, W. R. (2011). *cis*-Antisense RNA, another level of gene regulation in bacteria. *Microbiol Mol Biol Rev* **75**, 286–300.

Hill, S. A., Samuels, D. S., Carlson, J. H., Wilson, J., Hogan, D., Lubke, L. & Belland, R. J. (1997). Integration host factor is a transcriptional cofactor of *pilE* in *Neisseria gonorrhoeae*. *Mol Microbiol* **23**, 649–656.

Hoe, C. H., Raabe, C. A., Rozhdestvensky, T. S. & Tang, T. H. (2013). Bacterial sRNAs: regulation in stress. *Int J Med Microbiol* **303**, 217–229.

Kellogg, D. S., Cohen, I. R., Norins, L. C., Schroeter, A. L. & Reising, G. (1968). *Neisseria gonorrhoeae* II. Colonial variation and pathogenicity during 35 months *in vitro*. *J Bacteriol* **96**, 596–605.

Koomey, M., Bergstrom, S., Blake, M. & Swanson, J. (1991). Pilin expression and processing in pilus mutants of *Neisseria gonorrhoeae*: critical role of Gly_{-1} in assembly. *Mol Microbiol* **5**, 279–287.

Marzi, S., Fechter, P., Chevalier, C., Romby, P. & Geissmann, T. (2008). RNA switches regulate initiation of translation in bacteria. *Biol Chem* **389**, 585–598.

Masters, T. L., Wachter, S., Wachter, J. & Hill, S. A. (2016). H-NS suppresses pilE intragenic transcription and antigenic variation in *Neisseria gonorrhoeae*. *Microbiology* **162**, 177–190.

Pannekoek, Y., Huis in 't Veld, R., Hopman, C. T., Langerak, A. A., Speijer, D. & van der Ende, A. (2009). Molecular characterization and

identification of proteins regulated by Hfq in *Neisseria meningitidis*. *FEMS Microbiol Lett* **294**, 216–224.

Ramsey, M. E., Bender, T., Klimowicz, A. K., Hackett, K. T., Yamamoto, A., Jolicoeur, A., Callaghan, M. M., Wassarman, K. M., van der Does, C. & Dillard, J. P. (2015). Targeted mutagenesis of intergenic regions in the *Neisseria gonorrhoeae* gonococcal genetic island reveals multiple regulatory mechanisms controlling type IV secretion. *Mol Microbiol* **97**, 1168–1185.

Régnier, P. & Arraiano, C. M. (2000). Degradation of mRNA in bacteria: emergence of ubiquitous features. *BioEssays* **22**, 235–244.

Schuck, A., Diwa, A. & Belasco, J. G. (2009). RNase E autoregulates its synthesis in *Escherichia coli* by binding directly to a stem-loop in the *rne* 5′ untranslated region. *Mol Microbiol* **72**, 470–478.

Sittka, A., Pfeiffer, V., Tedin, K. & Vogel, J. (2007). The RNA chaperone Hfq is essential for the virulence of *Salmonella typhimurium*. *Mol Microbiol* **63**, 193–217.

Swanson, J. (1973). Studies on gonococcus infection. IV. Pili: their role in attachment of gonococci to tissue culture cells. *J Exp Med* **127**, 571–589.

Swanson, J. (1982). Colony opacity and protein II compositions of gonococci. *Infect Immun* **37**, 359–368.

Swanson, J., Robbins, K., Barrera, O., Corwin, D., Boslego, J., Ciak, J., Blake, M. & Koomey, J. M. (1987). Gonococcal pilin variants in experimental gonorrhea. *J Exp Med* **165**, 1344–1357.

Tønjum, T. & Koomey, M. (1997). The pilus colonization factor of pathogenic neisserial species: organelle biogenesis and structure/function relationships – a review. *Gene* **192**, 155–163.

Uppal, S., Akkipeddi, V. S. & Jawali, N. (2008). Posttranscriptional regulation of *cspE* in *Escherichia coli*: involvement of the short 5′-untranslated region. *FEMS Microbiol Lett* **279**, 83–91.

Wachter, J. & Hill, S. A. (2015). Small transcriptome analysis indicates that the enzyme RppH influences both the quality and quantity of sRNAs in *Neisseria gonorrhoeae*. *FEMS Microbiol Lett* **362**, 1–7.

Wachter, J., Masters, T. L., Wachter, S., Mason, J. & Hill, S. A. (2015). *pilS* loci in *Neisseria gonorrhoeae* are transcriptionally active. *Microbiology* **161**, 1124–1135.

Wade, J. T. & Grainger, D. C. (2014). Pervasive transcription: illuminating the dark matter of bacterial transcriptomes. *Nat Rev Microbiol* **12**, 647–653.

Waters, L. S. & Storz, G. (2009). Regulatory RNAs in bacteria. *Cell* **136**, 615–628.

Zuker, M. (2003). Mfold web server for nucleic acid folding and hybridization prediction. *Nucleic Acids Res* **31**, 3406–3415.

Edited by: P. W. O'Toole and D. Grainger